

Supporting Information for

Cooperative Chloride Hydrogel Electrolytes Enabling Ultralow-Temperature Aqueous Zinc Ion Batteries by the Hofmeister Effect

Changyuan Yan¹, Yangyang Wang¹, Xianyu Deng^{1,*}, Yonghang Xu^{2,*}

¹Shenzhen Key Laboratory of Advanced Materials, School of Materials Science and Engineering, Harbin Institute of Technology, Shenzhen, 518055, China

²School of Materials Science and Hydrogen Energy, Foshan University, Foshan, 528000, China

*Corresponding authors. E-mail: xydeng@hit.edu.cn (Xianyu Deng); yonghangxu@fosu.edu.cn (Yonghang Xu)

Supplementary Figures

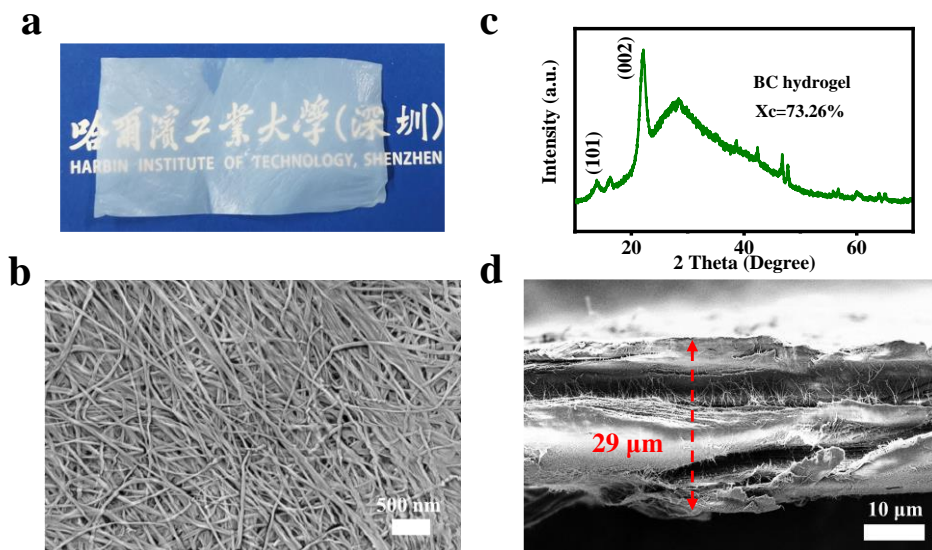


Fig. S1 Optical image (**a**), SEM image (**b**), XRD pattern (**c**) and cross-sectional SEM image (**d**) of the BC hydrogel

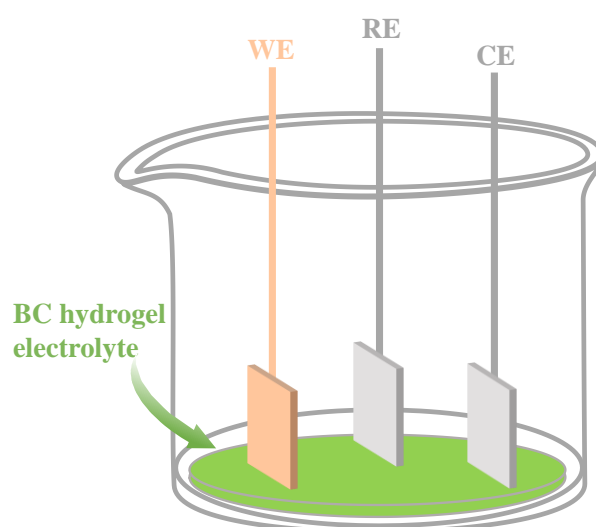


Fig. S2 The three-electrodes configuration for measuring the electrochemical windows of the electrolytes

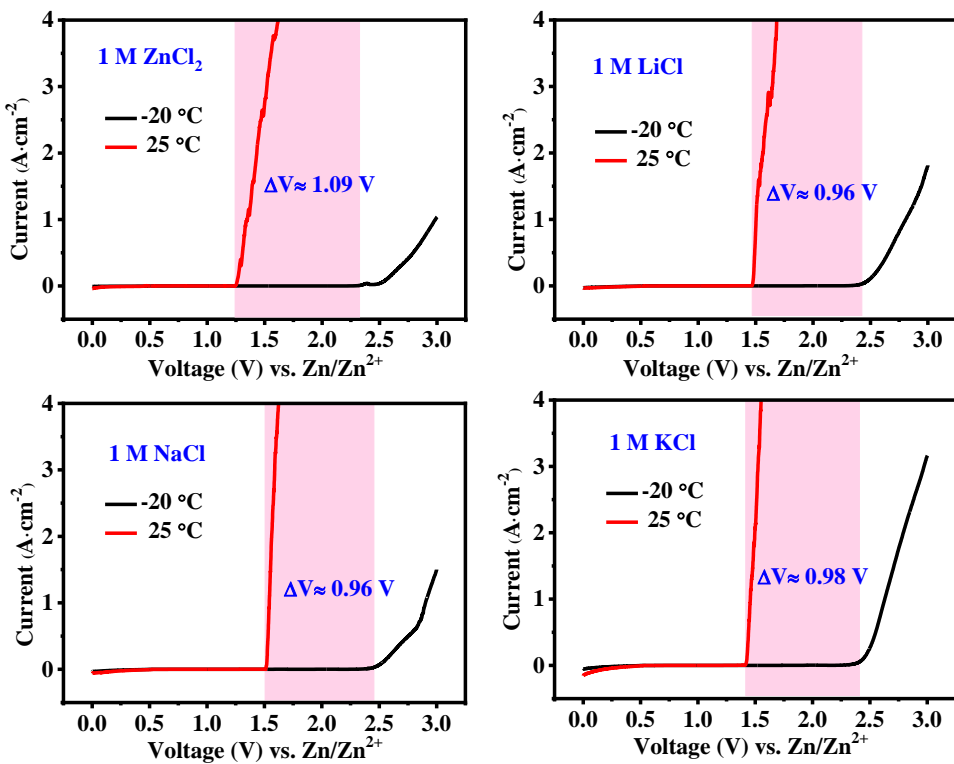


Fig. S3 The electrochemical windows of hydrogel electrolytes containing 1 M ZnCl₂, 1 M LiCl, 1 M NaCl and 1 M KCl at 25 °C and -20 °C, respectively

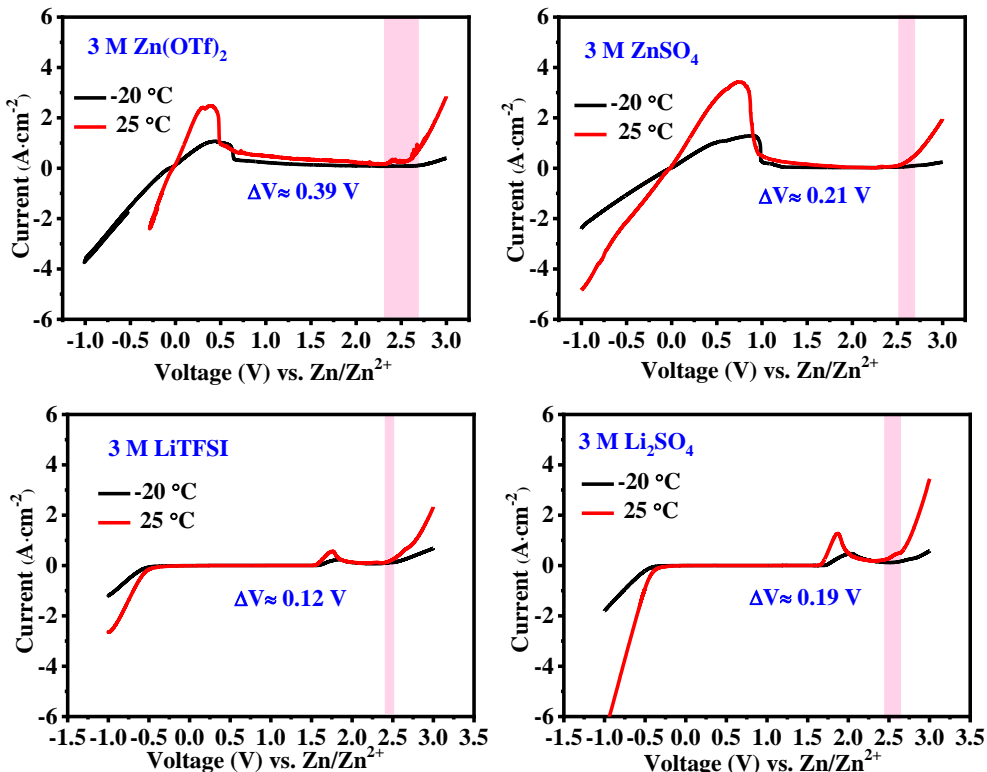


Fig. S4 The electrochemical windows of hydrogel electrolytes containing 3 M Zn(OTf)₂, 3 M ZnSO₄, 3 M LiTFSI and 3 M Li₂SO₄ at 25 °C and -20 °C, respectively

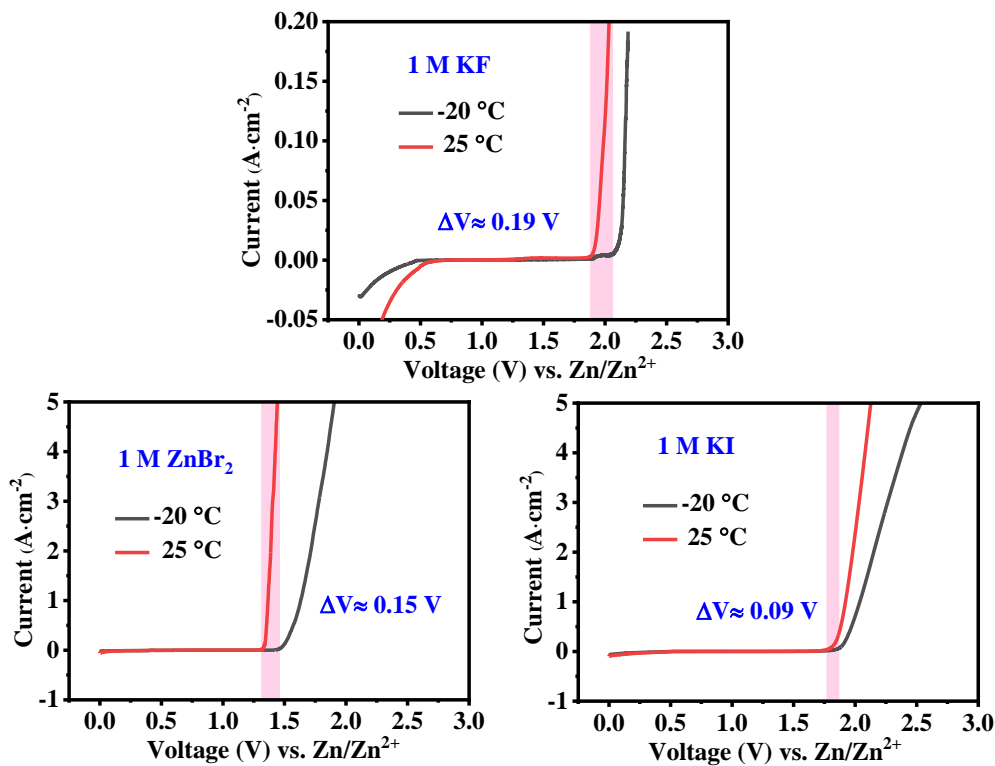


Fig. S5 The electrochemical windows of hydrogel electrolytes containing 1 M KF, 1 M ZnBr₂, 1 M KI at 25 °C and -20 °C, respectively

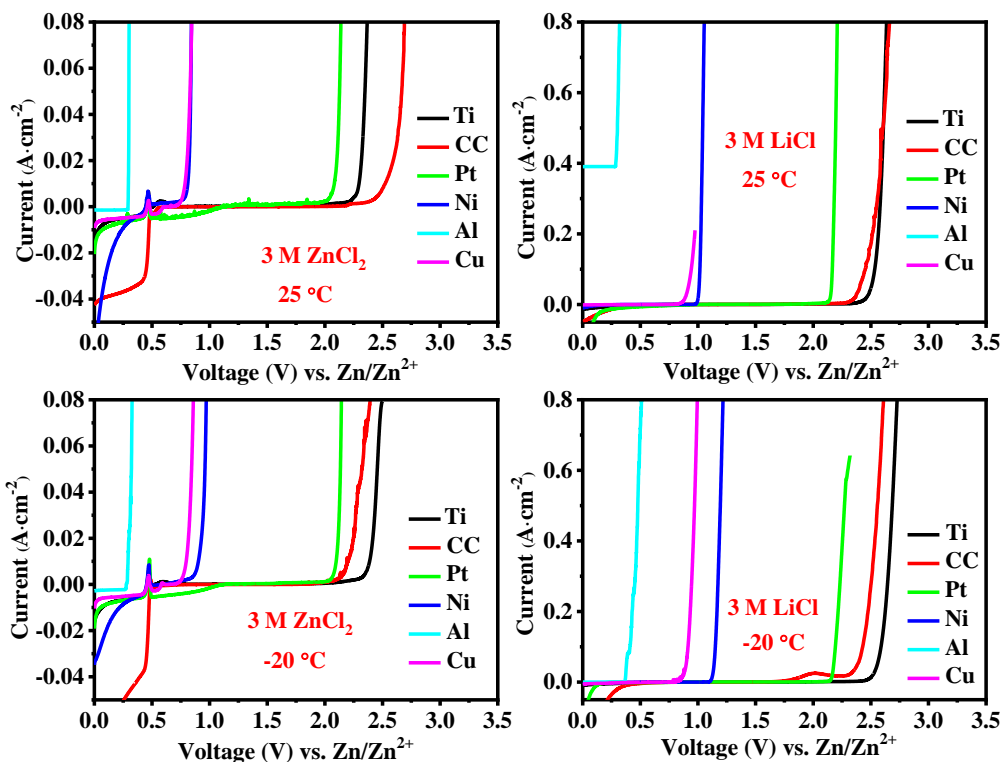


Fig. S6 The electrochemical windows of 3 M ZnCl₂ and 3 M LiCl hydrogel electrolytes based on different working electrodes at 25 °C and -20 °C, respectively

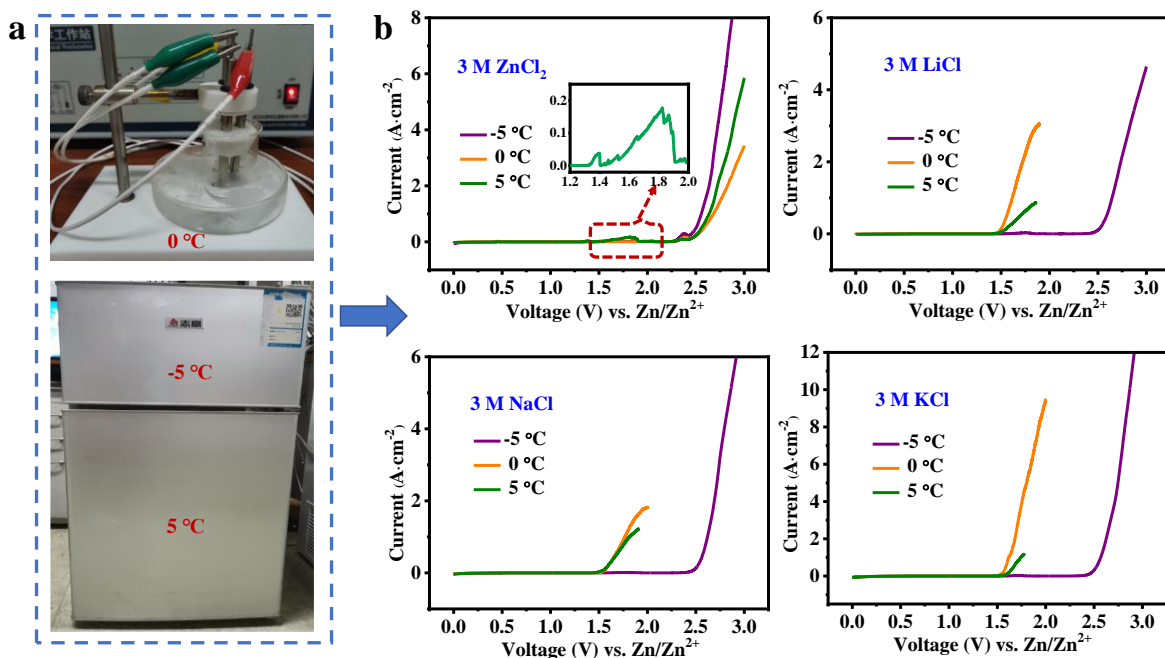


Fig. S7 (a) The temperature control devices ($5\text{ }^{\circ}\text{C}$, $0\text{ }^{\circ}\text{C}$ and $-5\text{ }^{\circ}\text{C}$). (b) The electrochemical windows of hydrogel electrolytes containing 3 M ZnCl_2 , 3 M LiCl , 3 M NaCl and 3 M KCl at $5\text{ }^{\circ}\text{C}$, $0\text{ }^{\circ}\text{C}$ and $-5\text{ }^{\circ}\text{C}$, respectively

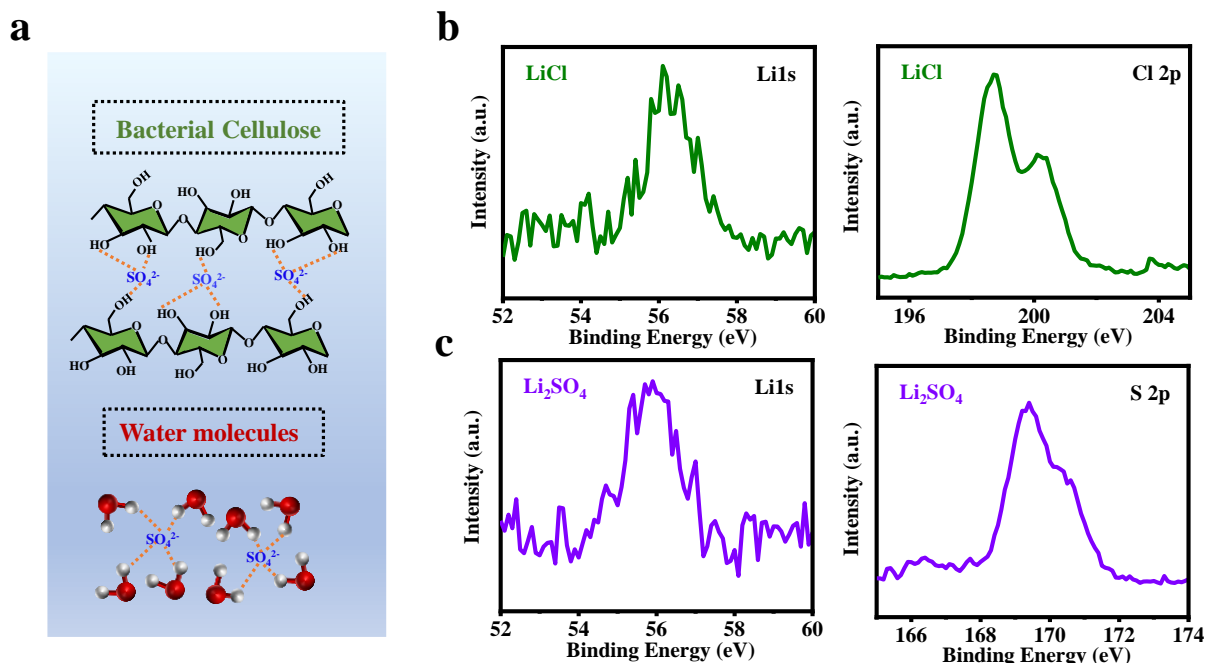


Fig. S8 (a) Schematic diagram of the H-bond formation between SO_4^{2-} and bacterial cellulose/water molecules. (b) XPS spectra for 3 M LiCl hydrogel electrolyte (Li 1s and Cl 2p). (c) XPS spectra for 3 M Li_2SO_4 hydrogel electrolyte (Li 1s and S 2p)

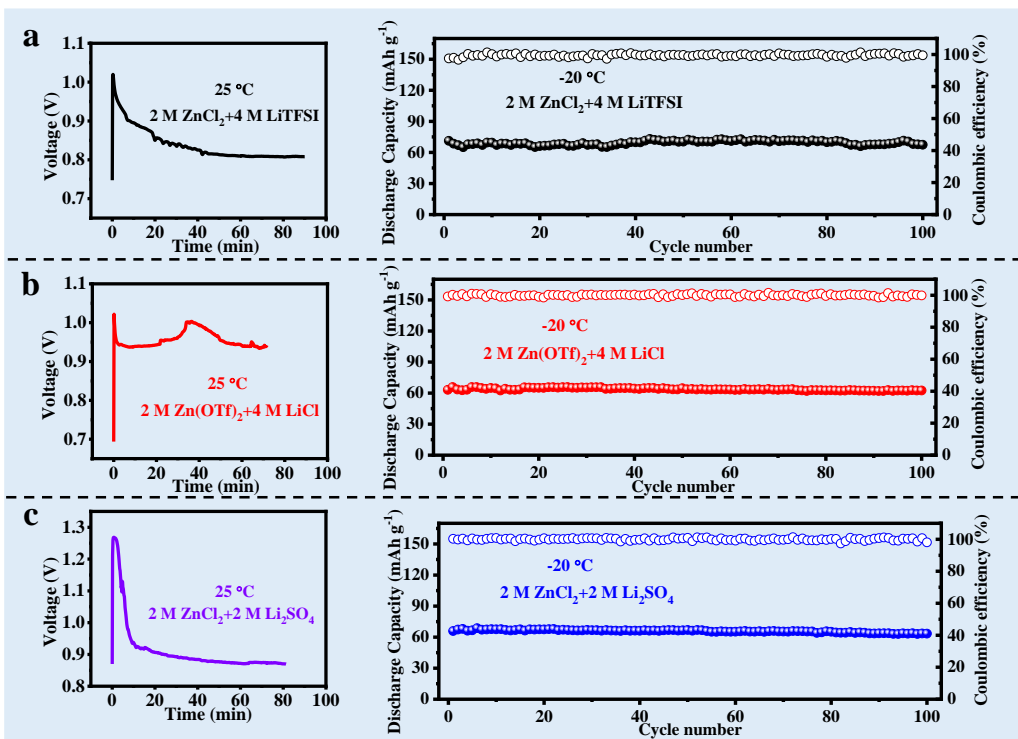


Fig. S9 GCD tests of the LiFePO₄/Zn cells using hydrogel electrolytes with 2 M Zn²⁺ and 4 M Li⁺ (2 M ZnCl₂+4 M LiTFSI **(a)**, 2 M Zn(OTf)₂+4 M LiCl **(b)**, and 2 M ZnCl₂+2 M Li₂SO₄ **(c)**) at 25 °C and -20 °C, respectively (0.2 A g⁻¹)

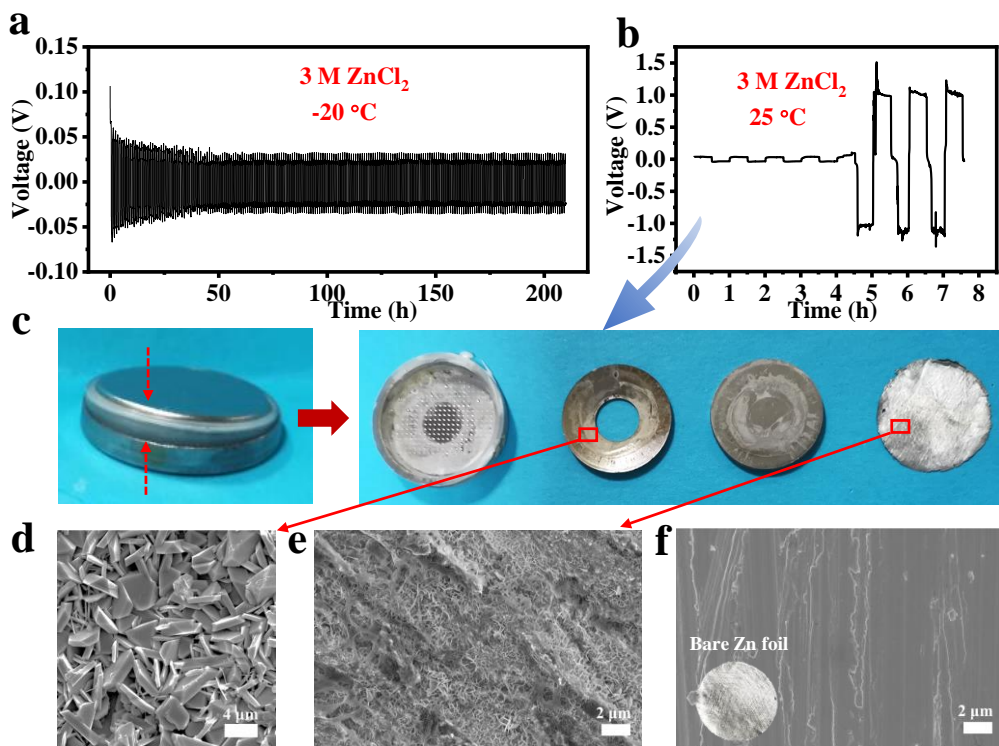


Fig. S10 The voltage profiles of symmetric Zn/Zn cell with 3 M ZnCl₂ hydrogel electrolyte at -20 °C **(a)** and 25 °C **(b)**, respectively (0.2 mA cm⁻²). Optical photographs **(c)**, SEM images of the spring **(d)** and Zn anode **(e)** from the corresponding Zn/Zn cell after cycling at 25 °C. **(f)** SEM image of bare Zn foil (the inset is the optical image)

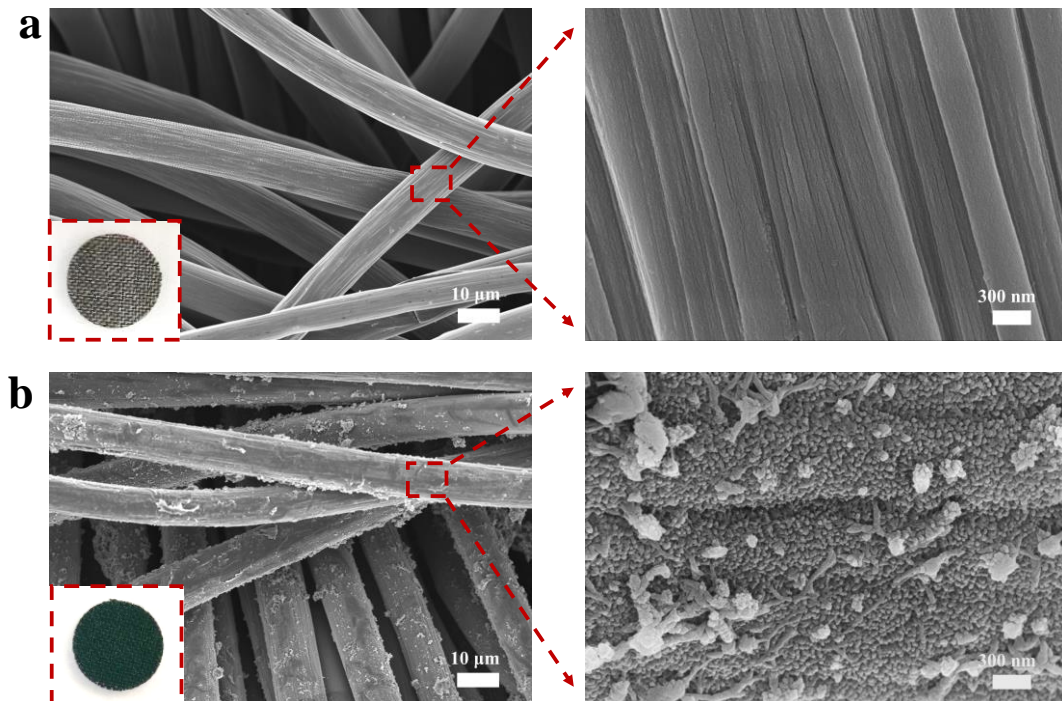


Fig. S11 SEM images of carbon cloth (**a**) and PANI/carbon cloth (**b**). Insets are the corresponding optical images

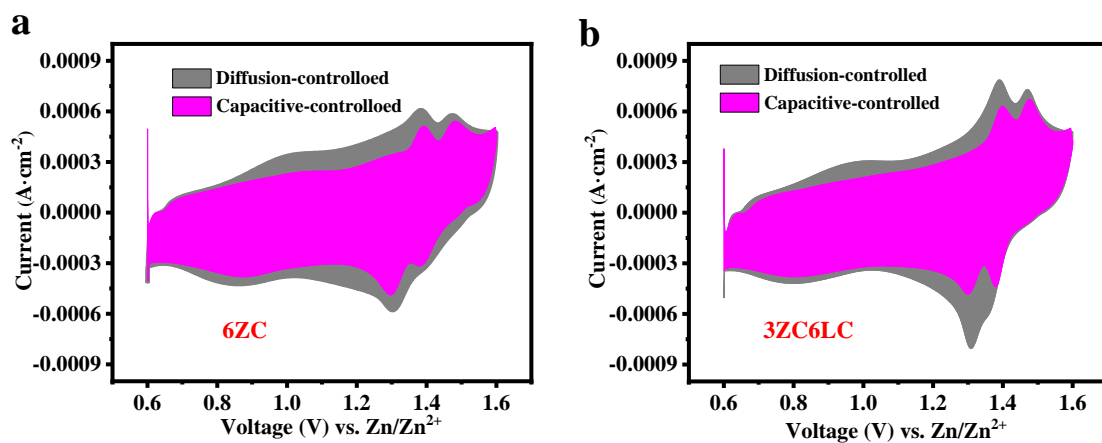


Fig. S12 Capacitive-controlled and diffusion-controlled contributions of PANI/Zn batteries based on 6ZC (**a**) and 3ZC6LC (**b**) at a scan rate of 1 mV s⁻¹ (-30 °C)

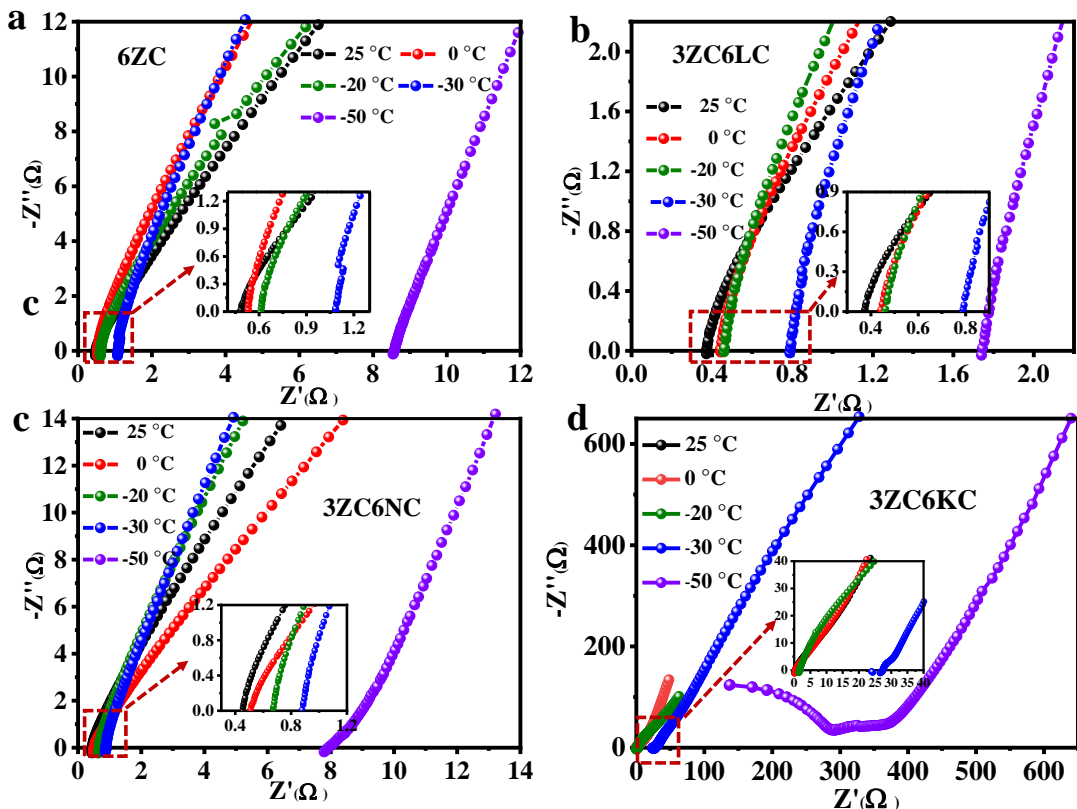


Fig. S13 EIS spectra of the symmetric SS/SS system based on 6ZC (a), 3ZC6LC (b), 3ZC6NC (c) and 3ZC6KC (d) measured at different temperatures

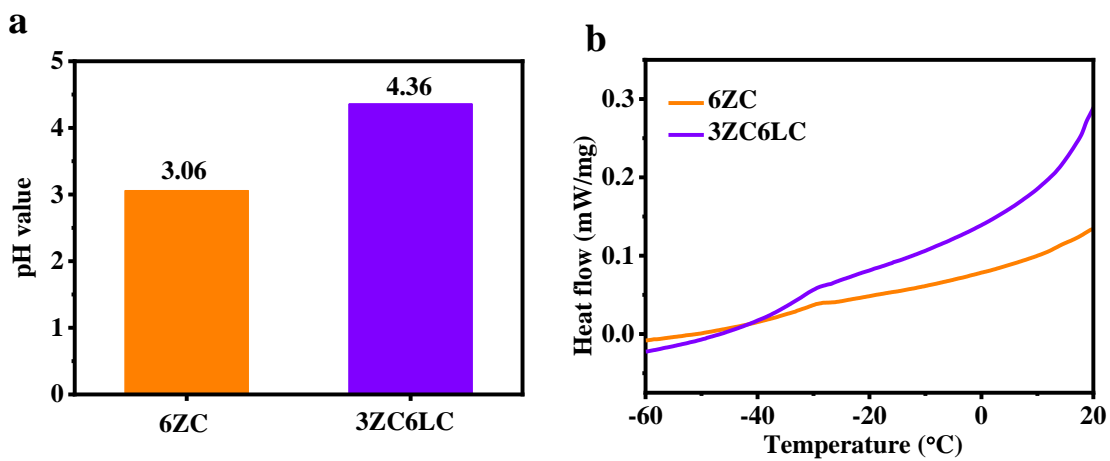


Fig. S14 The pH values (a) and DSC curves (b) of 6ZC and 3ZC6LC

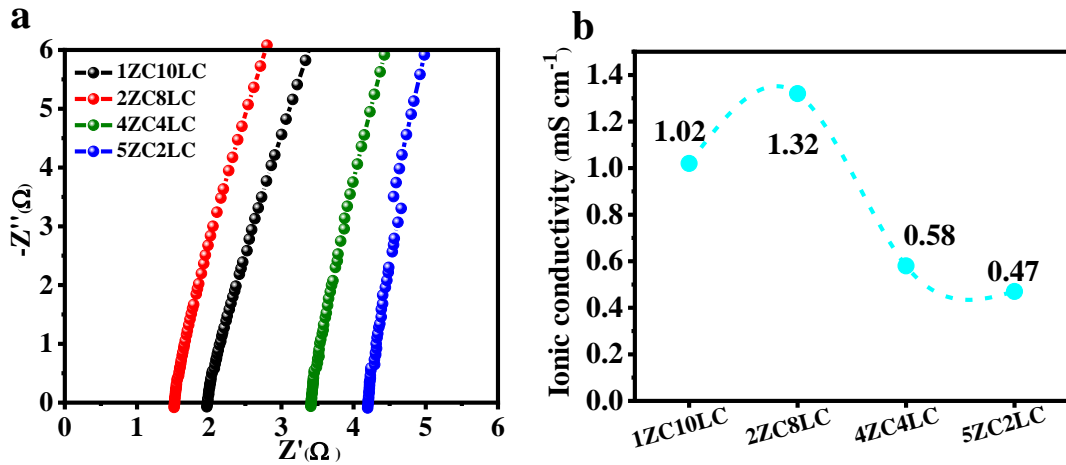


Fig. S15 (a) EIS spectra of the symmetric SS/SS system based on 1 M ZnCl₂+10 M LiCl, 2 M ZnCl₂+8 M LiCl, 4 M ZnCl₂+4 M LiCl and 5 M ZnCl₂+2 M LiCl hydrogel electrolytes at -50 °C (denoted 1ZC10LC, 2ZC8LC, 4ZC4LC and 5ZC2LC, respectively). (b) The ionic conductivity of corresponding hydrogel electrolytes

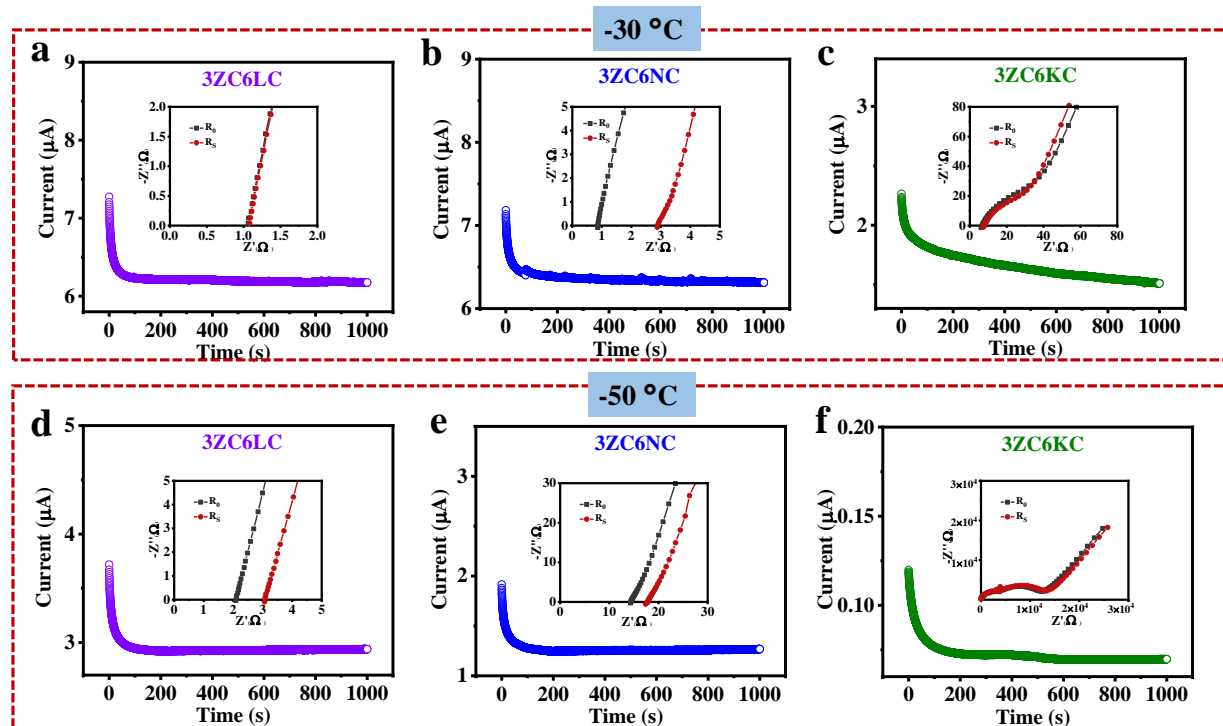


Fig. S16 Current-time curves at -30 °C (**a-c**) and -50 °C (**d-f**) of symmetric Zn/Zn cells following a voltage of 10 mV for 1000 s. Insets are the corresponding EIS spectra before and after polarization

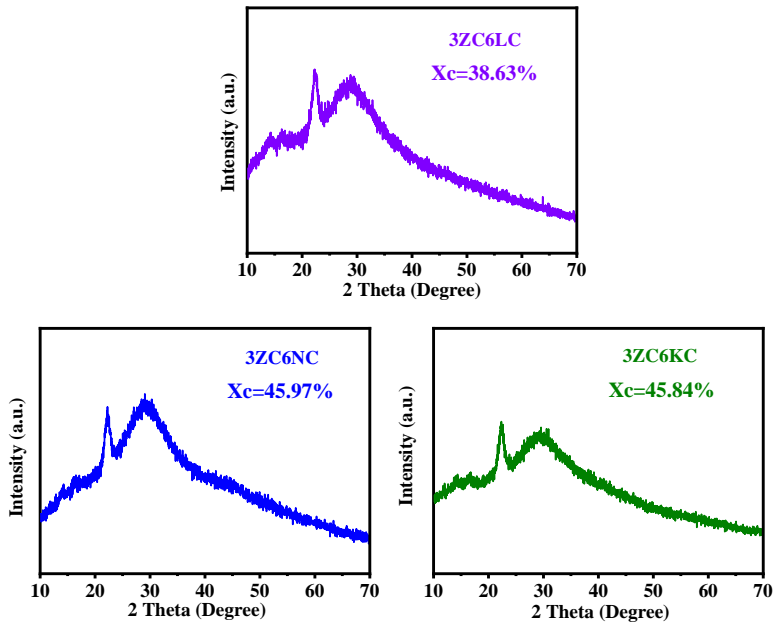


Fig. S17 XRD patterns of 3ZC6LC, 3ZC6NC and 3ZC6KC

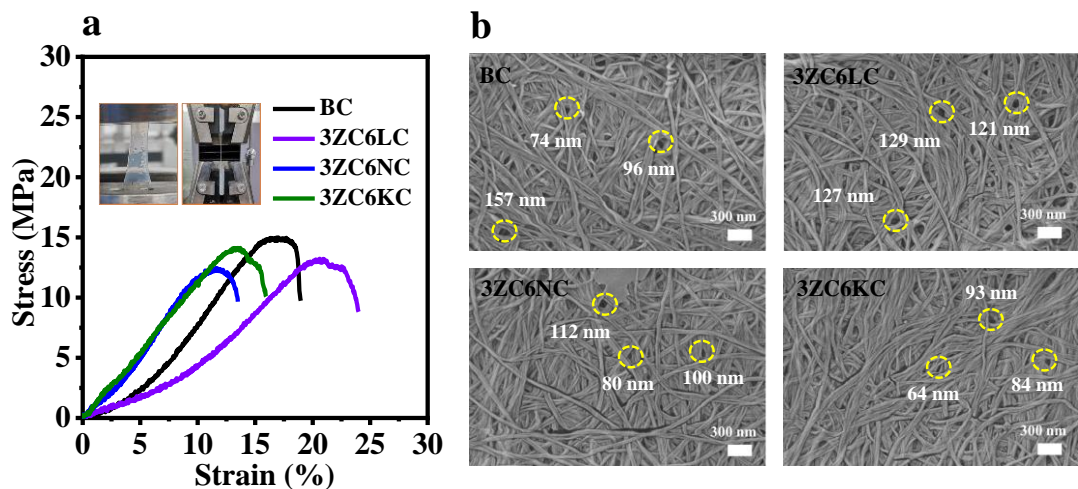


Fig. S18 (a) Stress–strain curves of BC, 3ZC6LC, 3ZC6NC and 3ZC6KC. (b) SEM images of corresponding hydrogel electrolytes after immersing in deionized water for 12 h

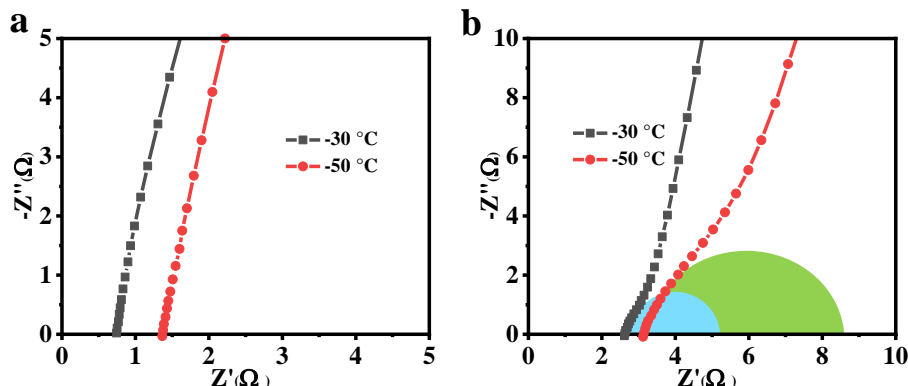


Fig. S19 EIS spectra of Zn/Zn (a) and PANI/Zn (b) cells with 3ZC6LC before testing

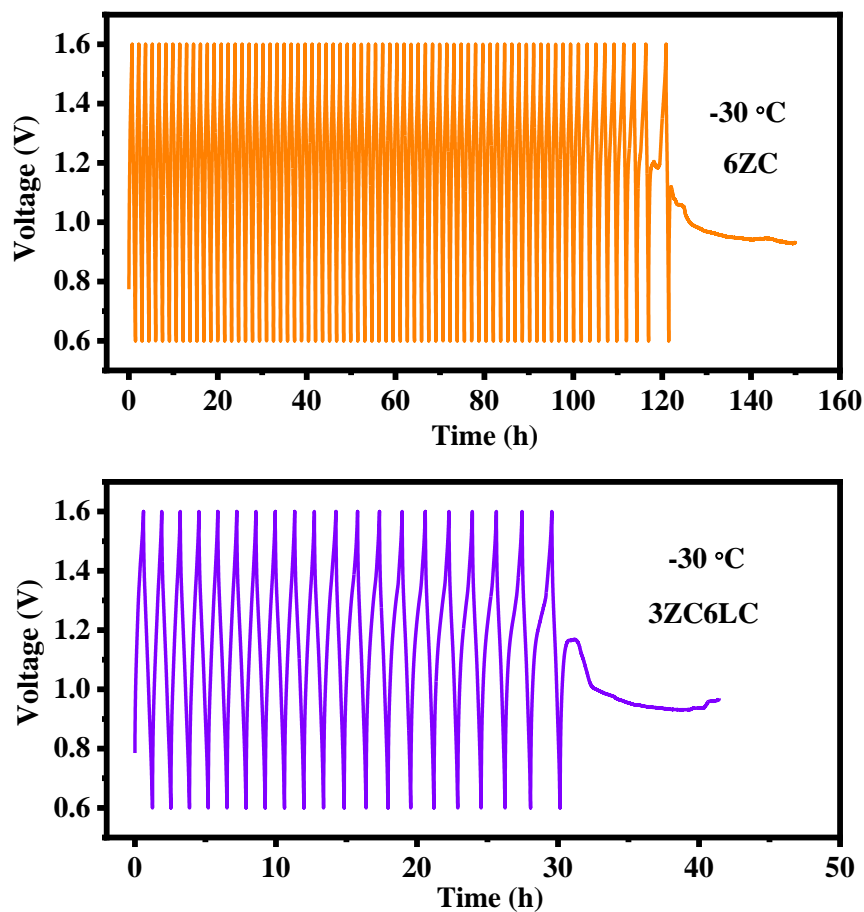


Fig. S20 The voltage profiles of PANI/Zn cells with 6ZC and 3ZC6LC at -30 °C and 0.2 A g⁻¹

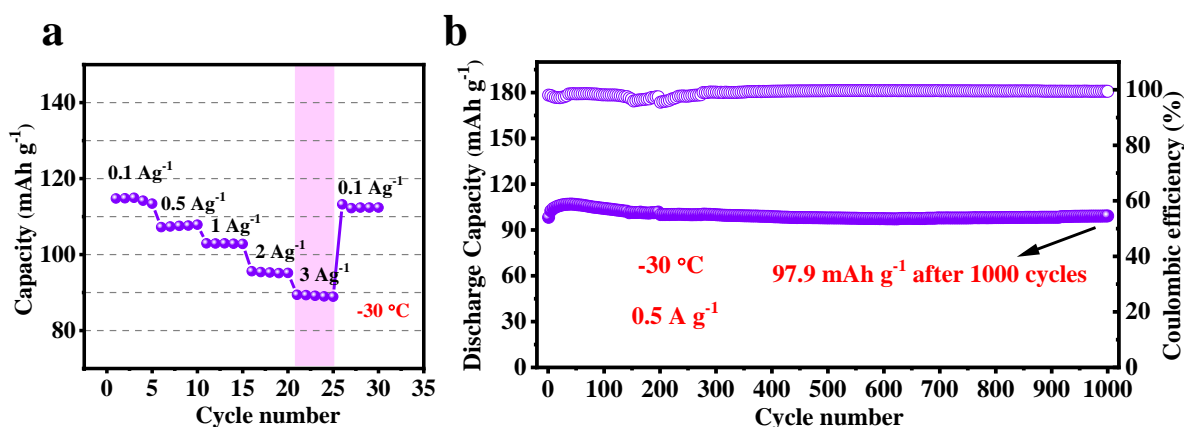


Fig. S21 Rate performance (**a**) and cycling performance (**b**) of the PANI/Zn cell with high mass loading (~3 mg cm⁻²) by using 3ZC6LC at -30 °C

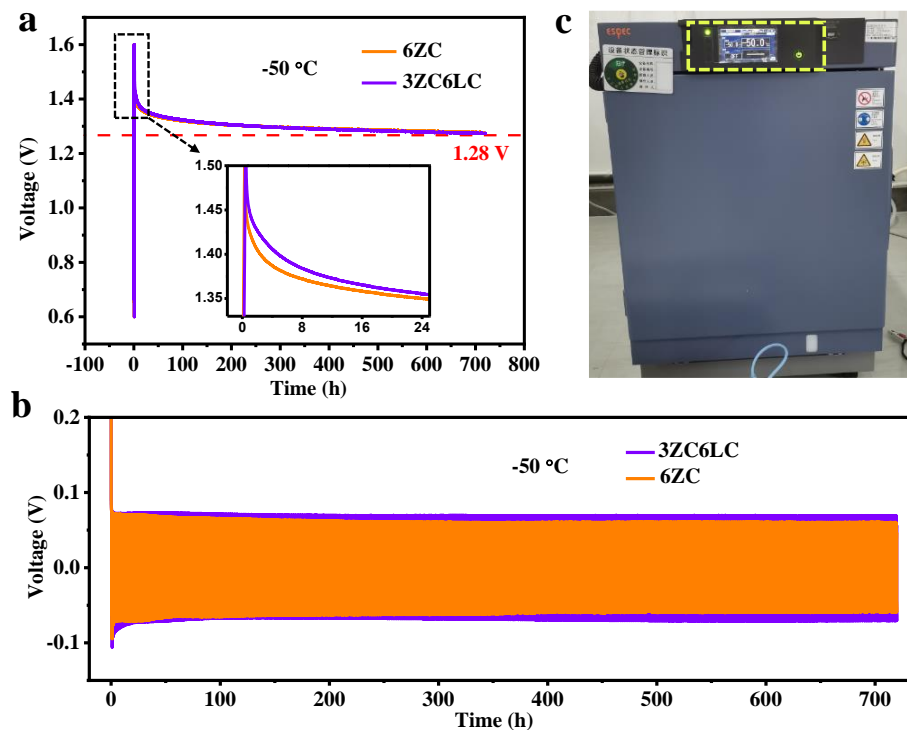


Fig. S22 (a) The self-discharge curves of PANI/Zn cell with 6ZC and 3ZC6LC at -50 °C (30 days). (b) The voltage profiles of symmetric Zn/Zn cell with 6ZC and 3ZC6LC at -50 °C and 0.2 mA cm⁻² (30 days). (c) The temperature control equipment (-50 °C)

Table S1 The electrochemical windows of 3 M ZnCl₂ and 3 M LiCl hydrogel electrolytes at different working electrodes

Working electrodes	3 M ZnCl ₂		3 M LiCl	
	25 °C	-20 °C	25 °C	-20 °C
stainless steel	1.26 V	2.39 V	1.20 V	2.51 V
Al	0.27 V	0.28 V	0.29 V	0.37 V
Cu	0.73 V	0.75 V	0.84 V	0.85 V
Ni	0.76 V	0.84 V	0.98 V	1.09 V
Pt	2.02 V	2.04 V	2.09 V	2.14 V
CC	2.41 V	2.16 V	2.26 V	2.29 V
Ti	2.22 V	2.32 V	2.32 V	2.46 V

Table S2 Calculation of transference numbers from analysis of polarization experiments at low temperatures

Electrolyte	Temperature(°C)	ΔV(mV)	R ₀ (Ω)	R _s (Ω)	I ₀ (μA)	I _s (μA)	t ⁺
3ZC6LC	-30	10	1.06	1.08	7.28	6.18	0.85
3ZC6NC	-30	10	0.87	2.91	7.19	6.32	0.88
3ZC6KC	-30	10	45.09	47.22	2.27	1.51	0.66
3ZC6LC	-50	10	2.09	3.06	3.72	2.94	0.79
3ZC6NC	-50	10	14.36	17.74	1.92	1.27	0.66
3ZC6KC	-50	10	13967	14911	0.12	0.07	0.52

Table S3 Comparison of low-temperature performance of PANI/Zn batteries with other electrolytes reported in the literatures

Cathode material	Electrolyte	Operating temperature	Cycle life	Capacity	Ref.
PANI	2 M ZnSO ₄ + 50 v/v% methanol	-10 °C	89.3% after 2000 cycles at 1 A g ⁻¹	100.8 mAh g ⁻¹	[S1]
PANI	1 M ZnCl ₂ +0.5 M NH ₄ Cl+50 wt% EG	-20 °C	99.8% after 150 cycles at 1 A g ⁻¹	73.9 mAh g ⁻¹	[S2]
PANI	7.5 m ZnCl ₂	-70 °C	100% after 2000 cycles at 0.2 A g ⁻¹	84.9 mAh g ⁻¹	[S3]
PANI	3 M ZnCl₂+6 M LiCl	-50 °C	100% after 2000 cycles at 0.5 A g⁻¹	96.5 mAh g⁻¹	This work

Supplementary References

- [S1] Q. Zhang, K. Xia, Y. Ma, Y. Lu, L. Li, J. Liang, S. Chou, J. Chen, Chaotropic anion and fast-kinetics cathode enabling low-temperature aqueous Zn batteries, ACS Energy Lett. **6**(8) (2021) 2704-2712. <https://doi.org/10.1021/acsenergylett.1c01054>
- [S2] Z. Cong, W. Guo, P. Zhang, W. Sha, Z. Guo, C. Chang, F. Xu, X. Gang, W. Hu, X. Pu, Wearable antifreezing fiber-shaped Zn/PANI batteries with suppressed Zn dendrites and operation in sweat electrolytes, ACS Appl. Mater. Interfaces **13**(15) (2021) 17608-17617. <https://doi.org/10.1021/acsami.1c02065>
- [S3] Q. Zhang, Y. Ma, Y. Lu, L. Li, F. Wan, K. Zhang, J. Chen, Modulating electrolyte structure for ultralow temperature aqueous zinc batteries, Nat. Commun. **11**(1) (2020) 4463. <https://doi.org/10.1038/s41467-020-18284-0>